Volume 1 | Number 1 | Jan 2013 | Pages 1–100

Green Chemistry

Cutting-edge research for a greener sustainable future

www.rsc.org/greenchem

Stille couplings in water @RT

ROYAL SOCIETY OF CHEMISTRY

ROYAL SOCIETY OF CHEMISTRY

www.rsc.org/greenchem

Green Chemistry

ARTICLE

Biomanufacturing of CdS quantum dots

Zhou Yang,[a] Li Lu,[b] Victoria F. Bernard,[a] Qian He,[b] Christopher J. Kiely,[b] Bryan W. Berger,[a,]* Steven McIntosh[a,]*

Nature provides powerful but as-yet largely unharnessed methods for low-cost, green synthesis of inorganic functional materials such as quantum dots. These materials have diverse applications from medicine to renewable energy. Harnessing nature's unique ability to achieve cost effective and scalable manufacturing solutions with reduced environmental impact is integral to realizing a future biomanufacturing economy. To address this challenge, a bacterial strain has been engineered to enable biosynthesis of CdS nanocrystals with extrinsic crystallite size control in the quantum confinement range. This strain yields extracellular, water-soluble quantum dots from low-cost precursors at ambient temperatures and pressure. The biomanufacturing approach demonstrated here produces CdS semiconductor nanocrystals with associated size-dependent band gap and photoluminescent properties.

Introduction

Semiconductor quantum dots (QDs) have numerous potential applications in a number of technologies, including display technologies, *in vivo* or *in vitro* biomedical imaging/detection, and quantum-dot solar cells.[1–6] Most current methods to produce CdS QDs utilize elevated temperature, organic solvent based processes. For example, the method of Murray et al. utilizes bis(trimethylsilyl)sulfide [(TMS)$_2$S] reacting with dimethylcadmium [Me$_2$Cd] at 300°C in an anhydrous environment.[7] Note that Me$_2$Cd is expensive, toxic, and pyrophoric. The alternative method of Peng and Peng utilizes trioctylphosphine oxide [TOPO], CdO, and hexylphosphonic acid or tetradecylphosphonic acid at 300 $^\circ$C, again in anhydrous environment.[8] The reported figure of merit, quantum yields (QYs), of the resulting CdS quantum dots vary in the range 3-12%.[9,10] In addition to environmental issues related to scale-up of these solvent based reactions, the reactants themselves must be synthesized. As such there has been increasing interest in developing aqueous based synthesis methods, commonly based on reactions of cadmium sulfate [CdSO$_4$] with, for example, sodium thiosulphate [Na$_2$S$_2$O$_3$][11] or sodium sulfide [Na$_2$S].[12]

Biosynthesis and assembly of hard materials, including QDs, has been described previously in both prokaryotes and eukaryotes.[13–21] Both have evolved several resistance mechanisms in response to toxic levels of heavy metals such as cadmium. These responses include the production of cysteine-rich peptides to direct growth of insoluble metal precipitates[17,22]

and the formation of glutathione-metal complexes to trap intracellular metals.[20,23] These observations have inspired the pursuit of a range of biological approaches to semiconductor nanocrystal biosynthesis, including using peptides, glutathione or other cellular components to direct synthesis.[17,18,20,24–31] For example, Li *et al.*, produced a single size of CdSe QDs within yeast cells through genetic engineering of intracellular redox conditions, illustrating the potential for cellular engineering to regulate nanocrystal biosynthesis.[32]

While this and several other biological approaches have shown that biomineralization of CdS and related semiconductor nanocrystals can occur, these previous methods demonstrate only limited control over the final particle size or production of particles with a limited size distribution. Since the opto-electronic functionality of QDs is largely due to their size dependent band gap, any application relevant synthesis route must allow reproducible control over the nanocrystal size within the quantum confinement size range.

Bai *et al.* utilized immobilized *Rhodobacter sphaeroides* to demonstrate a progressive increase in CdS particle size with increasing cell incubation time, but did not provide information on the size distribution of the particles or the evolution of particle size over time.[33] Other reports of biosynthesized CdS nanocrystals show broad size distributions for single growth times. For example, Borovaya synthesized CdS particles with sizes ranging from 2 to 8 nm within a single growth batch.[28]

These previous reports demonstrate a mixture of both intracellular QDs[18,26,30,31] and extracellular QD[27–29,34]

Green Chemistry Accepted Manuscript
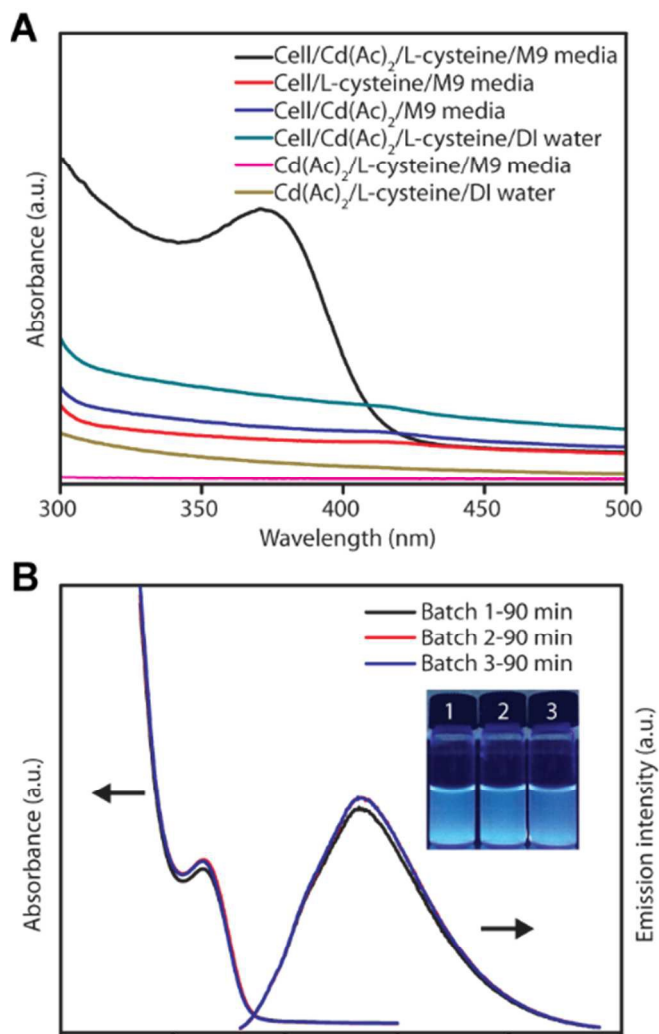
Fig. 1. Absorption and emission spectra of the as-grown cultures. (A) Absorption spectra of a series of samples prepared using different growth conditions, showing that only SMCD1 cells grown in the presence of both cadmium acetate and L-cysteine in M9 minimal media result in the formation of CdS QDs with a well-defined first excitonic peak. (B) Optical properties of three different batches of CdS QDs prepared using the same growth conditions showing good reproducibility. Inset is a photograph of the culture supernatants illuminated under UV light. The emission spectra were recorded using a 350 nm excitation wavelength.

production. Extracellular production is preferable as it removes a requirement for cell lysis during harvesting, decreasing protein and other biomacromolecule contamination of the product nanocrystals. However, no previous report has demonstrated reproducible, extracellular biomanufacturing of CdS QDs.

In this work, we describe a novel alternative aqueous-based, bacteria mediated, biosynthetic procedure for CdS nanocrystal synthesis at 37 °C. We utilize the relatively inexpensive precursor cadmium acetate [$Cd(CH_3CO_2)_2$] as a Cd source and the amino acid L-cysteine as the sulphur source and capping agent. The resulting quantum dots show QYs approaching those of the chemical synthesized materials.

A distinguishing feature of this work is the demonstration of reproducible CdS nanocrystal biosynthesis with control over the mean particle size largely in the 2-4 nm range, providing access to a wide range of quantum confined band gap energies. While the mean size and distribution width increases with increasing growth time, the as-synthesized standard deviation in mean size is demonstrated to be still less than 1 nm. This was achieved by utilizing directed evolution to engineer a strain of *Stenotrophomonas maltophilia* (SMCD1) that is capable of extracellular production of CdS nanocrystals to simplify purification. *Stenotrophomonas maltophilia* was specifically chosen because of its intrinsically high resistance to a variety of heavy metals, including cadmium.[35,36] The nanocrystals produced are confirmed to be crystalline CdS via high resolution scanning transmission electron microscopy, X-ray energy dispersive spectroscopy (XEDS), and X-ray diffraction.

Results and Discussion

Stenotrophomonas maltophilia was isolated from soil using previously described methods and iteratively selected for variants in culture that were tolerant to cadmium acetate at concentrations in excess of 1 mmol.[37] Cadmium-tolerant colonies were selected from cadmium-containing plates, and cultures grown in M9 minimal media containing 8 mmol L-cysteine. From the observed photoluminescence (Table S1) and absorption spectra (Fig. 1A) with 6 h growth, only SMCD1 cells grown in the presence of both cadmium acetate and L-cysteine in M9 minimal media result in fluorescence consistent with the formation of CdS QDs with a well-defined first excitonic peak. Other combinations of ingredients lacking bacterium strain SMCD1, cadmium acetate or L-cysteine do not show any fluorescence, thus demonstrating that CdS formation and luminescence only occurs under culture conditions containing cadmium acetate, L-cysteine and SMCD1 cells. Furthermore, the procedure is reproducible, with essentially identical QD optical properties observed from independent cultures using optimized growth media and the same growth time (Fig. 1B).

Using the identified optimized growth conditions (Table S1), we find that photoluminescence is retained in the culture supernatants after removal of the cells by centrifugation, indicating that the water-soluble fluorescent particles are produced extracellularly (Fig. 2A). We also find that both absorption and fluorescence peaks shift systematically with increasing growth time in culture. Absorption spectra for samples with various growth times demonstrate well-defined first excitonic peaks (Fig. 2B) with maxima that shift to higher wavelengths with increasing growth time. The normalized fluorescence emission spectra (Fig. 2C) also show a shift to higher wavelength with increasing growth time. For the absorption spectra, the peak wavelength increases from 312 nm to 378 nm, while the corresponding emission spectra peak wavelength moves from 460 nm to 562 nm as the growth time is increased from 30 min up to 360 min.
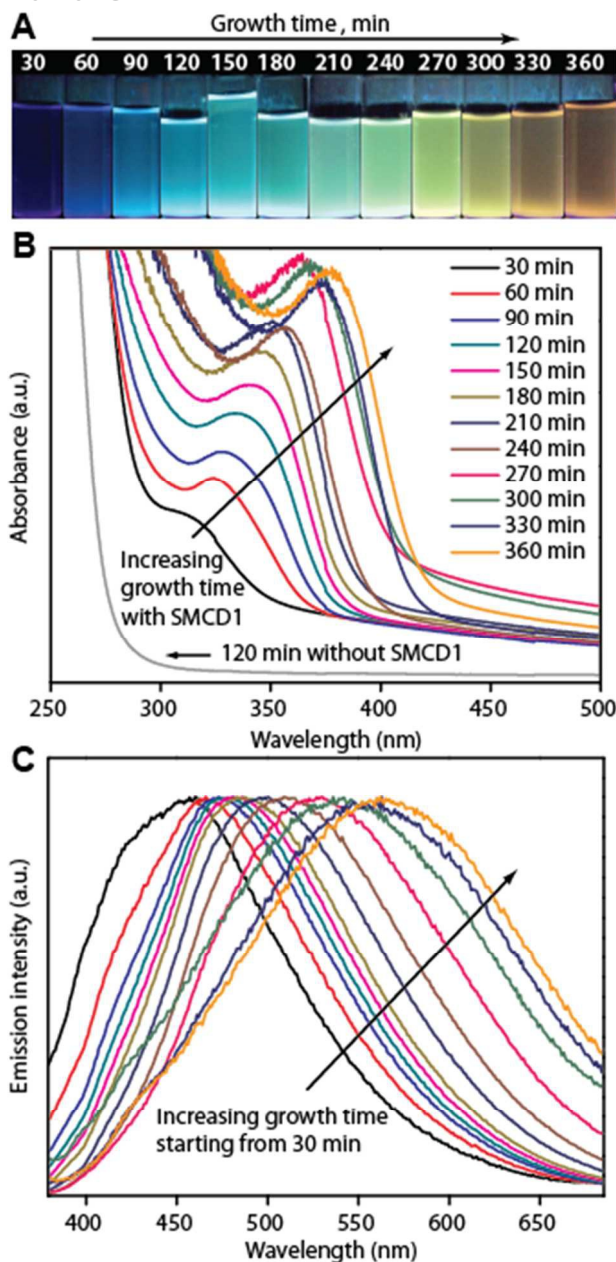
Fig. 2. Optical properties of the as-grown CdS QDs with different growth times. (A) Photograph of the culture supernatants from strain SMCD1 collected at various growth times when illuminated under UV light. (B) UV-vis absorption spectra of CdS QDs as a function of growth time. (C) Fluorescence emission spectra using a 350 nm excitation wavelength as a function of growth time.

While it may be hypothesized that another biosynthesized fluorescent species is responsible for the observed optical properties, all of this data is consistent with the biosynthetic formation of water soluble CdS quantum dots. Firstly, both cadmium acetate and L-cysteine are required for fluorescence to be observed in culture, indicating that the fluorescent species is CdS (Fig, 1 and Table S1). Secondly, strain SMCD1 growing in M9 minimal media is necessary for fluorescence to appear indicating that this bacterial strain facilitates the biomineralization of CdS (Fig, 1 and Table S1). Thirdly, the measured absorption wavelength maxima are consistent with a blue-shift from the bulk CdS band edge value (~515 nm) as expected for quantum confined CdS nanoparticles (Fig. 2B). The emission wavelengths are consistent with broad trap emission from such particles. Fourthly, the observed red-shift in both adsorption and emission wavelengths are consistent with increasing mean size of quantum confined particles with increasing time in culture (Fig. 2C). The relatively large Stokes shift is typical of L-cysteine capped CdS QDs in aqueous solution as reported previously.[38,39] It is likely that the as-produced QDs are capped with L-cysteine due to the relatively high L-cysteine concentration in the media, as well as the requirement of L–cysteine for synthesis.

Additional evidence to support biosynthesis of CdS QDs from strain SMCD1 was obtained by high resolution transmission electron microscopy (HRTEM) imaging of the resultant CdS QDs. Specifically, to evaluate the crystal structure and particle size distribution of the CdS materials, nanocrystals produced at a representative growth time of 60 min were purified and characterized by HRTEM (Fig. 3). The highly dispersed QDs are clearly observable (Fig. 3A) by phase contrast imaging. From electron diffraction (Fig. 3A, inset), two broad but distinct rings corresponding to interplanar spacings of 0.33 nm and 0.21 nm are observed, which are consistent with expected lattice spacings of CdS. However, selected area electron diffraction (SAED) cannot unequivocally distinguish between the possible CdS polymorphs (*i.e.* the zinc-blende and wurtzite type structures), as they both have lattice spacings similar to those measured within the limits of experimental error. X-ray powder diffraction patterns (Fig. 4) were also collected and are consistent with CdS formation; however peak broadening due to the nanoscopic nature of the particles results in just two major broad peaks from which again the exact polymorphic structures present cannot be distinguished.

Green Chemistry Accepted Manuscript
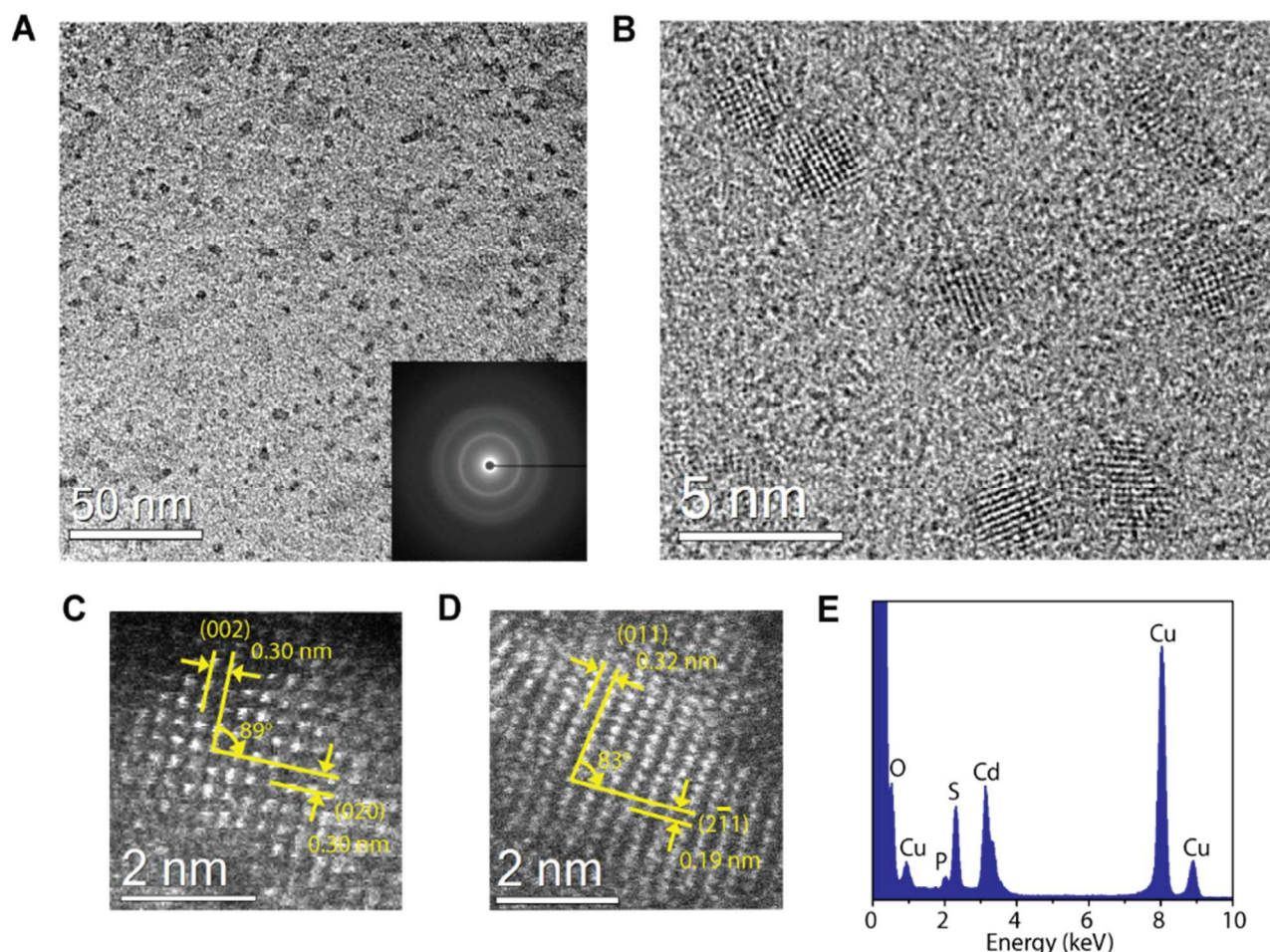
Fig. 3. Electron microscopy characterization of purified CdS QDs after 60 min growth. (A) Bright field TEM image of CdS QDs illustrating the typical particle dispersion, inset in (A) is the corresponding selected area electron diffraction (SAED) pattern. (B) Representative high resolution TEM image of CdS QDs. (C and D) High angle annular dark field (HAADF) images of particles exhibiting zinc-blende and wurtzite type structures respectively. (E) Energy-dispersive X-ray spectroscopy (XEDS) analysis confirming the co-existence of Cd and S in the QDs.
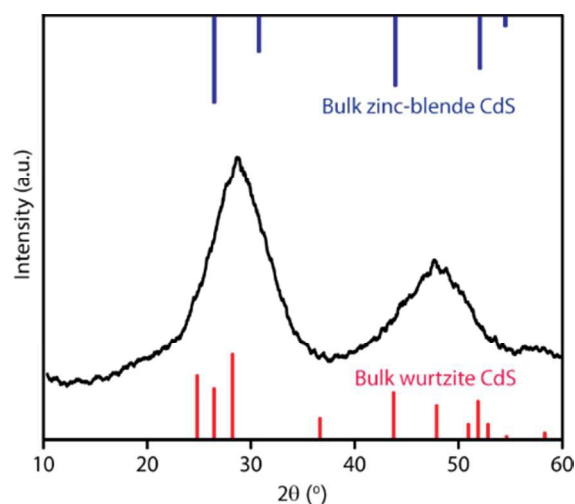
HRTEM and STEM-HAADF (high angle annular dark field) images were acquired to obtain more localized crystallographic information from the biosynthesized QDs. The HRTEM (Fig. 3B) and STEM-HAADF images (Fig. 3, C and D) exhibit lattice fringes within individual particles, whose spacings and intersection angles are consistent in some particles with the sphalerite form of CdS whereas in others they match the wurtzite form. The measured d-spacing value of 0.30 nm (Fig. 3C) for the two planes indicated match those of the (002) and (020) planes in zinc-blende type CdS viewed along the [100] projection; the measured interplanar angle is 89°, which matches the expected 90° angle between these two planes. In Fig. 3D the measured d-spacing values of 0.19 nm and 0.32 nm corresponds to those of the ($2\bar{1}1$) plane and (011) plane of wurtzite-type CdS, respectively; the measured interplanar angle between these two planes is 83°, which is also consistent with the expected value of 82.0° calculated from the cross product of ($2\bar{1}1$) and (011) when viewed along [$\bar{1}\bar{1}1$]. Therefore, we conclude that both zinc-blende and wurtzite type structures co-exist for CdS QDs produced by strain SMCD1. X-ray energy dispersive spectroscopy (XEDS) analysis confirmed that the

particles are primarily comprised of cadmium and sulfur (Fig. 3E); some traces of phosphorus and oxygen are also present, most likely due to residual phosphate from the M9 minimal growth media; the copper peaks are artefacts of the TEM support grid.
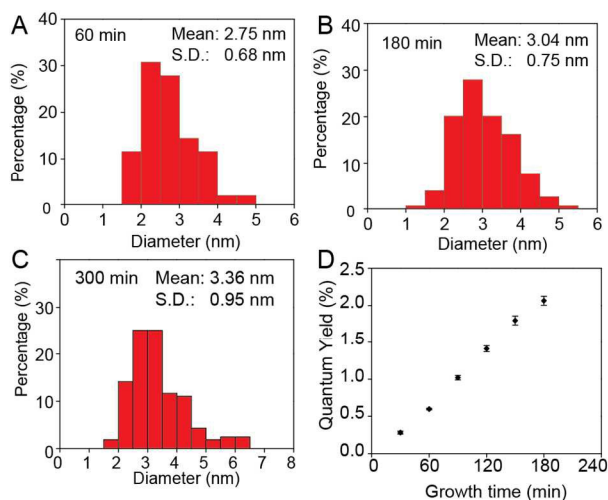
Particle size distributions (Fig. 5, A, B, and C) after 60, 180 and 300 min growth times were determined from analysis of such phase contrast images. The mean particle size increases from 2.75 to 3.04 to 3.36 nm after 60, 180 and 300 min, respectively. The breadth of the distribution also increases with increasing growth time with the standard deviation increasing from 0.68 to 0.95 nm between 60 and 300 min growth. The observed relationship between size and adsorption peak wavelength are in-line with other reports for L-cysteine capped CdS QDs.[38,40]

The quantum yields (QY) of the purified CdS QDs which had growth times ranging from 30 min to 180 min were found to exhibit an approximately linear increase from 0.30 % to 2.08 % (Fig. 5D). Determination of the QY at longer growth times was inaccurate due to aggregation of the larger particles. The range of measured QY is once again consistent with other

reports for l-cysteine capped QDs in aqueous solution and most importantly are about three orders of magnitude greater than the QY (0.007 %) reported for previous biosynthetic CdS QDs.[18] The relatively low QY as compared to more standard inorganic preparation methods may be due to quenching by the l-cysteine or the dimer cystine.[41,42] Taking into account the measured systematic variation in particle size distribution with growth time, it can be concluded that the QY monotonically increases with increasing mean nanocrystal size in the 30-180 min growth time range. Similar size-dependent trends for the photoluminescence QY of semiconductor nanocrystals have been noted previously.[43–47] As the particle size decreases, the surface-to-volume ratio increases, which results in a higher proportion of surface defects. Therefore, it is likely that non-radiative relaxation at surface traps become more important with decreasing particle size.

CdS QDs generated from SMCD1 show an extracellular growth period following cluster nucleation. In yeast, the removal of intracellular cadmium occurs through a glutathione-dependent mechanism, in which up-regulation of glutathione monomer, oligomer and cysteine-rich binding peptide biosynthesis occurs to neutralize cadmium through the formation of metal-thiol complexes.[23] Decomposition of bound thiol ligands, in this case the thiol group on L-cysteine, is thought to provide a source of sulfur for the CdS nanocrystal nucleation and growth. L-cysteine is one of three amino required for glutathione biosynthesis, and the rate of L-cysteine biosynthesis is typically limiting in terms of the overall cellular glutathione biosynthesis rate.[48]

To further investigate the CdS growth mechanism, we investigated particle growth following the removal of the bacterial cells from culture via centrifugation (Fig. 6). The optical density at 600 nm (OD_{600}) of the supernatant, a measure
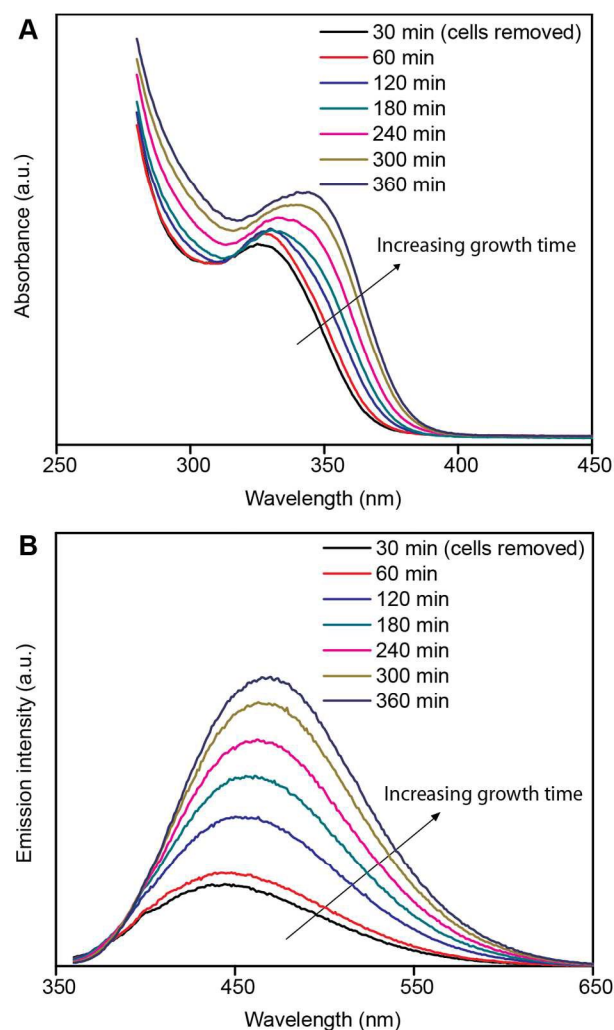

Fig. 4. X-ray powder diffraction pattern of the precipitated CdS quantum dot powder after X mins of growth. The stick patterns show the expected standard peak positions of the bulk wurtzite (bottom, PDF card no. 00-006-0314) and zinc-blende type CdS polymorphs (top, PDF card no. 00-010-0454).

Fig. 5. Particle size distributions and quantum yields of CdS QDs as a function of growth time. (A,B,C) Representative particle size distributions for growth times of 60, 180, and 300 min respectively (the mean values were derived from measurements of at least 100 particles). (D) Quantum yield values of CdS QDs with growth times ranging from 30 min to 180 min.

Fig. 6. Optical properties of the as-grown CdS QDs as a function of growth time in centrifuge supernatant following removal of cells via centrifugation at 30 minutes. (A) UV-vis absorption spectra (B) Fluorescence emission spectra using a 350 nm excitation wavelength as a function of growth time.

```
MSNATSQDRALALATLAIHGGQSPDPSTGAVMPPIYATSTYAQSSPGEHQGFEYSRTHNPTRFAYER CVASLEGGT RGFAFASGMAASS
TVIELLDDAGSHVVAMDDIYGGSFRLFERVRRTAGLDFSFVDLTDLAAFEASITPKTK MVWIETPTNPMLKIVDIAAVAAIAK RHGLIV
VVDNTFASPMLQRPLELGADLVLHSATKYLNGHSDMVGGMVVVGDNAELAEQMAFLQNSVGGVQGPFDSFLALRGLKTLPLRMKAHCAN
ALALAQWLEKHPAVEKVIYPGLASHPQHELAGH QMAGYGGIVSIVLK GGFDAAKRFCEKTELFTLAESLGGVESLVNHPAVMTHASIPV
AR REQLGISDALVR LSVGVEDLGDLQVDLGEALK
```

Fig. 7. Sequence of the Protein Associated with the QDs. The identified protein sequence (NCBI Accession Number WP_012509966), which corresponds to a predicted cystathionine beta-lyase, based on the results of ESI-MS is listed above. Specific peptide sequences from ESI-MS used in protein identification are given in bold and boxed for emphasis.

of cell concentration, after centrifugation was <2% of the initial value, confirming removal of the cells. The CdS QDs in the free supernatant continued to grow in the absence of cells, although at a slower rate as characterized by a smaller red-shift in both adsorption and fluorescence peak maxima with increasing growth time. For example, after 360 minutes the absorbance and fluorescence maxima are at 343 and 469 nm, respectively, without cells and at 378 and 562 nm, respectively, with cells. This result both confirms the extracellular production of the QDs, and indicates that QD growth does not require the continuous presence of cells throughout the entire growth process. We suggest that the presence of cells accelerates the rate of QD biosynthesis by continuously generating the extracellular components responsible for QD biosynthesis. Removal of the cells after an initial period reduces the rate of QD biosynthesis by reducing the concentration of extracellular components necessary for QD biosynthesis.

Interestingly, SDS-PAGE analysis of the supernatant does not show significant (>0.1-1.0 microgram detection limits) concentration of associated proteins or other biomacromolecules (Figure S1), indicating that the QDs are free in solution and not entrained in extracellular matrix or cell remnants. Many of the prior reports on this topic describe intercellular nanocrystals production requiring cell lysis prior to purification. This leads to association of proteins and other intracellular biomacromolecules on the nanocrystal surfaces at higher (>0.1-1.0 microgram) concentrations.[26,30,31]

In order to determine if low-abundance proteins or other biomacromolecules are associated with the biosynthetic QDs produced by the current method, the QD containing supernatant was dialyzed against distilled water to reduce the free Cd salt and L-cysteine concentration, lyophilized and analyzed by electrospray ionization mass spectrometry (ESI-MS). This technique is significantly more sensitive than the SDS-PAGE and revealed several proteins associate with the QDs that may be responsible for the observed extracellular CdS QD synthesis.

Of particular note, a putative cystathione gamma-lyase (NCBI Accession Number WP_012509966) was identified from independent QD samples analysed by ESI-MS (Figure 7). Cystathione gamma-lyases are a class of enzymes that produce H_2S from L-cysteine, and prior work has shown that overexpression of a highly active cystathione gamma-lyase in *E. coli* confers resistance to otherwise toxic concentrations (0.1-0.4 mM) of aqueous cadmium chloride by precipitation of bulk CdS through generation of H_2S from 1 mM L-cysteine.[49] Consistent with these results, we find that the presence of L-

cysteine is strictly required for QD biosynthesis from strain SMCD1 (Table S1 and Figure 1A).

In summary, all of our results point to a mechanism in which CdS QD biosynthesis occurs extracellularly via a cystathione gamma-lyase catalyzed conversion of L-cysteine to H_2S. This enzyme is produced in culture by strain SMCD1 and is found to be associated with the CdS QDs. Ongoing work is focusing on further elucidation of this mechanism.

Conclusions

We present a novel approach for the reproducible biosynthesis of extracellular, water-soluble CdS QDs using an engineered strain of *Stenotrophomonas maltophilia* (SMCD1) that has been specifically evolved to control particle size. Further ongoing optimization of the quality of these biosynthesised QDs, coupled with the use of low cost Cd and S sources, room temperature, and aqueous synthesis conditions will ultimately provide a route to low-cost, green synthesis of such CdS QDs. Thus, our biosynthetic approach to CdS QD production provides a viable pathway to realize the promise of green biomanufacturing of these materials for optoelectronic, energy, medicine and other emerging technological applications.

Experimental

Stenotrophomonas maltophilia was isolated from soil collected from the mountaintop campus of Lehigh University in Pennsylvania using previously described methods.[37] Strain identification was confirmed using 16S rRNA sequencing (SeqWright). Standard microbiology techniques were used for the growth and cultivation of *Stenotrophomonas maltophilia* using Luria-Bertani (LB) broth and M9 minimal media. Selection of cadmium resistant strains was performed iteratively in three steps by increasing the concentration of cadmium acetate: (1) Cultures were grown for 8-12 h at 37 °C in an orbital shaker in LB broth containing increasing concentrations of cadmium acetate (0.1~5 mM); (2) serial dilutions of cultures were plated onto LB-agar plates containing equivalent concentrations of cadmium acetate; and (3) individual colonies were isolated from plates. Cell growth rate in culture was measured by monitoring the change in optical density at 600 nm (OD_{600}). Colonies tolerant to cadmium acetate at concentrations in excess of 1 mM were selected from cadmium-containing plates. Using this selection procedure, we

isolated a specific strain (SMCD1) that exhibits continuous formation of luminescent particles

In a typical experiment, the selected SMCD1 were sub-cultured into LB broth (100 mL) and grown for 12 h at 37 °C with shaking. Cells were isolated by centrifugation and re-suspended in M9 minimal media (100 mL, OD$_{600}$=0.5). Then, cadmium acetate (1 mM) and L-cysteine (8 mM) were added and the mixture was placed in a 37 °C incubator with shaking. Sample aliquots were collected every 30 min, and CdS QDs separated from intact cells by centrifugation (5000 rpm), dialysis (Snakeskin 3500 MWCO; Thermo Pierce) with ultrapure, deionized water as the buffer and gravity-feed size exclusion chromatography (PD-10; Amersham).

In order to investigate the mechanism of particle growth, the same growth procedure was followed for 30 minutes growth time. At this point, the cell solution was centrifuged at 8000 rpm for ten minutes, reducing the optical density at 600 nm to 2% of the original value. The centrifuge supernatant was then returned to the incubator at 37 °C and sample aliquots were collected every 30 min.

One synthesized batch of QDs was separated from cells via centrifugation after 90 minutes of growth time. The supernatant was dialyzed against DI water for 24 hours prior to lyophilisation. The dry sample was analysed via electrospray ionization mass spectrometry.

The luminescence of purified QD suspensions was analyzed using a UV Bio-Rad Gel Doc 2000 system. Absorption spectra of QD suspensions were collected using an Ultrospec 3300 Pro (Amersham Biosciences). Fluorescence excitation and emission spectra for QD suspensions were collected using a Cary Eclipse Fluorescence Spectrophotometer (Varian). Room temperature photoluminescence quantum yields (PL QYs) were calculated using coumarin 1 in ethanol as a standard with a PL QY of 0.73.[50] Powder XRD measurements (Rigaku Miniflex II) were performed at room temperature by using Cu K$_{\alpha}$ (1.5418 Å) radiation.

For scanning transmission electron microscopy (STEM), selected area electron diffraction (SAED) and X-ray energy dispersive spectroscopy (XEDS) analysis, purified samples were prepared by drop casting the aqueous QD suspension onto a holey carbon-coated copper grid and allowing the liquid component to fully evaporate. The specimen was then analyzed in either (i) a 200kV aberration corrected JEOL ARM 200CF analytical electron microscope equipped with a Centurio XEDS system or (ii) a 200kV JEOL 2000FX conventional TEM equipped with an Oxford Instruments XEDS system.

Notes and references

[a] Department of Chemical and Biomolecular Engineering, Lehigh University, Bethlehem, PA 18015, USA.

[b] Department of Materials Science and Engineering, Lehigh University, Bethlehem, PA 18015, USA

* stm310@lehigh.edu (S.M.), bwb209@lehigh.edu (B.W.B.)

Electronic Supplementary Information (ESI) available: [Table of growth conditions from Figure 1A, Figure showing SDS-PAGE gel results].

1   K. Bourzac, *Nature*, 2013, **493**, 283.
2   K. Sanderson, *Nature*, 2009, **459**, 760–761.
3   A. P. Alivisatos, W. Gu and C. Larabell, *Annu. Rev. Biomed. Eng.*, 2005, **7**, 55–76.
4   P. Alivisatos, *Nat. Biotechnol.*, 2004, **22**, 47–52.
5   I. L. Medintz, H. T. Uyeda, E. R. Goldman and H. Mattoussi, *Nat. Mater.*, 2005, **4**, 435–446.
6   A. J. Nozik, M. C. Beard, J. M. Luther, M. Law, R. J. Ellingson and J. C. Johnson, *Chem. Rev.*, 2010, **110**, 6873–6890.
7   C. B. Murray, D. J. Norris and M. G. Bawendi, *J. Am. Chem. Soc.*, 1993, **115**, 8706–8715.
8   Z. A. Peng and X. Peng, *J. Am. Chem. Soc.*, 2001, **123**, 183–184.
9   D. Chen, F. Zhao, H. Qi, M. Rutherford and X. Peng, *Chem. Mater.*, 2010, **22**, 1437–1444.
10   J. S. Steckel, J. P. Zimmer, S. Coe-Sullivan, N. E. Stott, V. Bulović and M. G. Bawendi, *Angew. Chemie Int. Ed.*, 2004, **43**, 2154–2158.
11   C. Unni, D. Philip, S. L. Smitha, K. M. Nissamudeen and K. G. Gopchandran, *Spectrochim. Acta Part A Mol. Biomol. Spectrosc.*, 2009, **72**, 827–832.
12   M. Shao, F. Xu, Y. Peng, J. Wu, Q. Li, S. Zhang and Y. Qian, *New J. Chem.*, 2002, **26**, 1440–1442.
13   S. Mann, D. D. Archibald, J. M. Didymus, T. Douglas, R. Brigid, F. C. Meldrum, N. J. Reeves and B. R. Heywood, *Science*, 1993, **261**, 1286–1292.
14   C. Mao, C. E. Flynn, A. Hayhurst, R. Sweeney, J. Qi, G. Georgiou, B. Iverson and A. M. Belcher, *Proc. Natl. Acad. Sci. U. S. A.*, 2003, **100**, 6946–6951.
15   A. M. Belcher, X. H. Wu, R. J. Christensen, P. K. Hansma, G. D. Stucky and D. E. Morse, *Nature*, 1996, **381**, 56–58.
16   L. A. Bawazer, M. Izumi, D. Kolodin, J. R. Neilson, B. Schwenzer and D. E. Morse, *Proc. Natl. Acad. Sci. U. S. A.*, 2012, **109**, E1705–1714.
17   C. T. Dameron, R. N. Reese, R. K. Mehra, A. R. Kortan, P. J. Carroll, M. L. Steigerwald, L. E. Brus and D. R. Winge, *Nature*, 1989, **338**, 596–597.
18   S. H. Kang, K. N. Bozhilov, N. V Myung, A. Mulchandani and W. Chen, *Angew. Chem. Int. Ed. Engl.*, 2008, **47**, 5186–5189.
19   S. R. Stürzenbaum, M. Höckner, A. Panneerselvam, J. Levitt, J-S. Bouillard, S. Taniguchi, L-A. Dailey, R. Ahmad Khanbeigi, E. V Rosca, M. Thanou, K. Suhling, A. V Zayats and M. Green, *Nat. Nanotechnol.*, 2013, **8**, 57–60.
20   R. Y. Sweeney, C. Mao, X. Gao, J. L. Burt, A. M. Belcher, G. Georgiou and B. L. Iverson, *Chem. Biol.*, 2004, **11**, 1553–1559.
21   R. Cui, H-H. Liu, H-Y. Xie, Z-L. Zhang, Y-R. Yang, D-W. Pang, Z-X. Xie, B-B. Chen, B. Hu and P. Shen, *Adv. Funct. Mater.*, 2009, **19**, 2359–2364.
22   J. W. Moreau, P. K. Weber, M. C. Martin, B. Gilbert, I. D. Hutcheon and J. F. Banfield, *Science*, 2007, **316**, 1600–1603.
23   R. K. Mehra and D. R. Winge, *J. Cell. Biochem.*, 1991, **45**, 30–40.
24   E. D. Spoerke and J. A. Voigt, *Adv. Funct. Mater.*, 2007, **17**, 2031–2037.
25   S. Arunkumar, S. Tamilselvan, T. Ashokkumar, R. Geetha, K. Govindaraju, V. Ganesh Kumar, G. Singaravelu and K. Vijai Anand, *Mater. Lett.*, 2014, **134**, 225–228.

26   C. Gallardo, J. P. Monrás, D. O. Plaza, B. Collao, L. A. Saona, V. Durán-Toro, F. A. Venegas, C. Soto, G. Ulloa, C. C. Vásquez, D. Bravo and J. M. Pérez-Donoso, *J. Biotechnol.*, 2014, **187**, 108–115.

27   A. K. Suresh, *Spectrochim. Acta Part A Mol. Biomol. Spectrosc.*, 2014, **130**, 344–349.

28   M. Borovaya, A. Naumenko, N. Matvieieva, Y. Blume and A. Yemets, *Nanoscale Res. Lett.*, 2014, **9**, 686.

29   G. Chen, B. Yi, G. Zeng, Q. Niu, M. Yan, A. Chen, J. Du, J. Huang and Q. Zhang, *Colloids Surfaces B Biointerfaces*, 2014, **117**, 199–205.

30   Z. Yan, J. Qian, Y. Gu, Y. Su, X. Ai. and S. Wu, *Mater. Res. Express*, 2014, **1**, 15401.

31   L. Tan, A. Wan and H. Li, *ACS Appl. Mater. Interfaces*, 2014, **6**, 18–23.

32   Y. Li, R. Cui, P. Zhang, B-B. Chen, Z-Q. Tian, L. Li, B. Hu, D-W. Pang and Z-X. Xie, *ACS Nano*, 2013, **7**, 2240–2248.

33   H. Bai, Z. Zhang, Y. Guo and W. Jia, *Nanoscale Res. Lett.*, 2009, **4**, 717–723.

34   C. L. Wang, P. C. Michels, S. C. Dawson, S. Kitisakkul, J. A. Baross, J. D. Keasling and D. S. Clark, *Appl. Environ. Microbiol.* , 1997, **63** , 4075–4078.

35   R. P. Ryan, S. Monchy, M. Cardinale, S. Taghavi, L. Crossman, M. B. Avison, G. Berg, D. van der Lelie and J. M. Dow, *Nat. Rev. Microbiol.*, 2009, **7**, 514–525.

36   D. Pages, J. Rose, S. Conrod, S. Cuine, P. Carrier, T. Heulin and W. Achouak, *PLoS One*, 2008, **3**, e1539–1544.

37   C. Bollet, A. Davin-Regli and P. De Micco, *Appl. Environ. Microbiol.*, 1995, **61**, 1653–1655.

38   A. Chatterjee, A. Priyam, S. K. Das and A. Saha, *J. Colloid Interface Sci.*, 2006, **294**, 334–342.

39   E. V Krupko, G. Y. Grodzyuk, Y. B. Khalavka, G. M. Okrepka and L. P. Shcherbak, *Theor. Exp. Chem.*, 2011, **47**, 101–107.

40   K. Mullaugh and G. Luther III, *J. Nanoparticle Res.*, 2011, **13**, 393–404.

41   D. P. S. Negi and T. I. Chanu, *Nanotechnology*, 2008, **19**, 465503.

42   S. Tamang, G. Beaune, I. Texier and P. Reiss, *ACS Nano*, 2011, **5**, 9392–9402.

43   J. Beato-López, C. Fernández-Ponce, E. Blanco, C. Barrera-Solano, M. Ramírez-del-Solar, M. Domínguez, F. García-Cozar and R. Litrán, *Nanomater. Nanotechnol.*, 2012, **2**, 1–10.

44   M. L. Mastronardi, F. Maier-Flaig, D. Faulkner, E. J. Henderson, C. Kübel, U. Lemmer and G. A. Ozin, *Nano Lett.*, 2012, **12**, 337–342.

45   J. Zhang, X. Wang, M. Xiao, L. Qu and X. Peng, *Appl. Phys. Lett.*, 2002, **81**, 2076–2078.

46   C. Dong and J. Ren, *Analyst*, 2010, **135**, 1395–1399.

47   W. W. Yu, L. Qu, W. Guo and X. Peng, *Chem. Mater.*, 2003, **15**, 2854–2860.

48   S. M. Deneke and B. L. Fanburg, *Am. J. Physiol.*, 1989, **257**, 163–167.

49   C. Wang, A. Lum, S. Ozuna, D. Clark and J. Keasling, *Appl. Microbiol. Biotechnol.*, 2001, **56**, 425–430.

50   J. Guilford, W. R. Jackon, C. Choi and W. R. Bergmark, *J. Phys. Chem.*, 1985, **89**, 294–300.